Supplementary Information (SI)

A Promising Strategy to Tune the Schottky Barrier of $MoS_{2(1-x)}Se_{2x}$/graphene Heterostructure by Asymmetric Se Doping

Jisong Hu,[a] Wangyang Duan,[a] Hua He,[a] Hui Lv,[ab] Chuyun Huang[ab] and Xinguo Ma*[ab]

[a] *School of Science, Hubei University of Technology, Wuhan 430068, China;*

[b] *Hubei Collaborative Innovation Center for High-efficiency Utilization of Solar Energy, Hubei University of Technology, Wuhan 430068, China;*

*Corresponding Authors**,** E-mail: maxg2013@sohu.com

1. MoS_2/Gr heterostructure

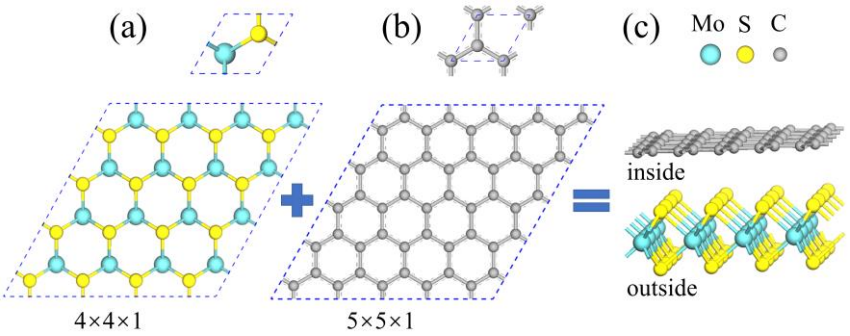

Figure S1. The stereo matching strategy of monolayer MoS_2 and graphene. Top views of (a) monolayer MoS_2 with 4×4×1 lateral periodicity and (b) graphene with 5×5×1 lateral periodicity; (c) Side view of MoS_2/Gr heterostructure.

2. Definition of vacancy formation energy

The vacancy formation energy required to remove a sulfur atom from the surface of monolayer MoS_2 is represented as:

$$E_V = E_T^q(Mo_nS_{2n-1}) + \mu_S - E_T^q(Mo_nS_{2n}) \quad (1)$$

where $E(Mo_nS_{2n-1})$ and $E(Mo_nS_{2n})$ are the total energies of the defective and stoichiometric slabs, respectively. The vacancy formation energy depends on growth conditions, which may be varied from S-rich to S-poor condition. For S-rich condition, cycle S_6 molecular is used to determine the chemical potential $\mu_S = \mu(S_6)/6$. However, for S-poor condition, the chemical potential of S element can be

expressed by $\mu_S = E(MoS_2) - \mu_{Mo}$, where $\mu_{Mo} = E(Mo_{bulk\ cell})/n$ and n is the number of Mo atom in bulk metal Mo. The formation energy of single S-vacancy is -2.928 eV for S-poor condition.

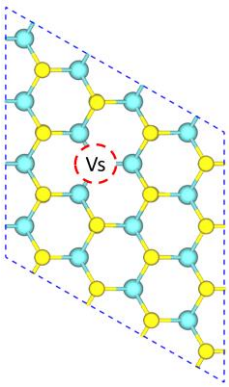

Figure S2. Top view of S-vacancy (red dashed line) pattern. The 4×4×1 supercell of monolayer MoS_2 is used to avoid the periodic interactions between the neighboring defects.

3. Energy band structures

The state-of-the-art hybrid DFT approach based on the Heyd-Scuseria-Ernzerhof functional (HSE06) was used to calculate the electronic structures of MoS_2 after geometric optimization. In the default hybrid functional HSE06, the screening parameter μ and the mixing parameter α are set as 0.21 $Å^{-1}$ and 0.25, respectively. And norm-conserving pseudopotentials were used for all-electron HSE06 calculations. The calculated band gap of monolayer MoS_2 is 2.23 eV at the high symmetry K point, which is slightly larger than the experimental band gap of about 1.80 eV.

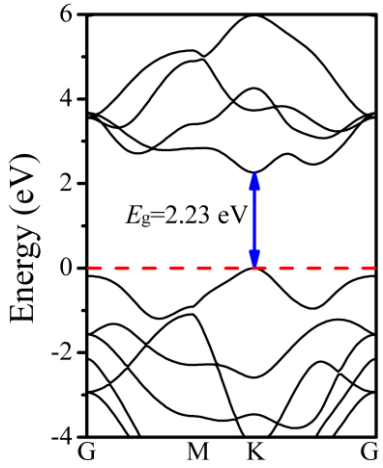

Figure S3. Energy band structures of monolayer MoS_2 using hybrid functional HSE06.

References

(1) J. Heyd, G. E. Scuseria, M. Ernzerhof, Hybrid Functionals Based on a Screened Coulomb Potential. *J. Chem. Phys.* 2003, **118**, 8207–8215.

(2) J. S. Lin, A. Qteish, M. C. Payne, V. Heine, Optimized and Transferable Nonlocal Separable Ab Initio Pseudopotentials. *Phys. Rev. B* 1993, **47**, 4174–4180.

(3) K. F. Mak, C. Lee, J. Hone, J. Shan, T. F. Heinz, Atomically Thin MoS_2: A New Direct-Gap Semiconductor. *Phys. Rev. Lett.* 2010, **105**, 2–5.

4. TDOS and PDOS of $MoS_{2(1-x)}Se_{2x}$/Gr heterostructure

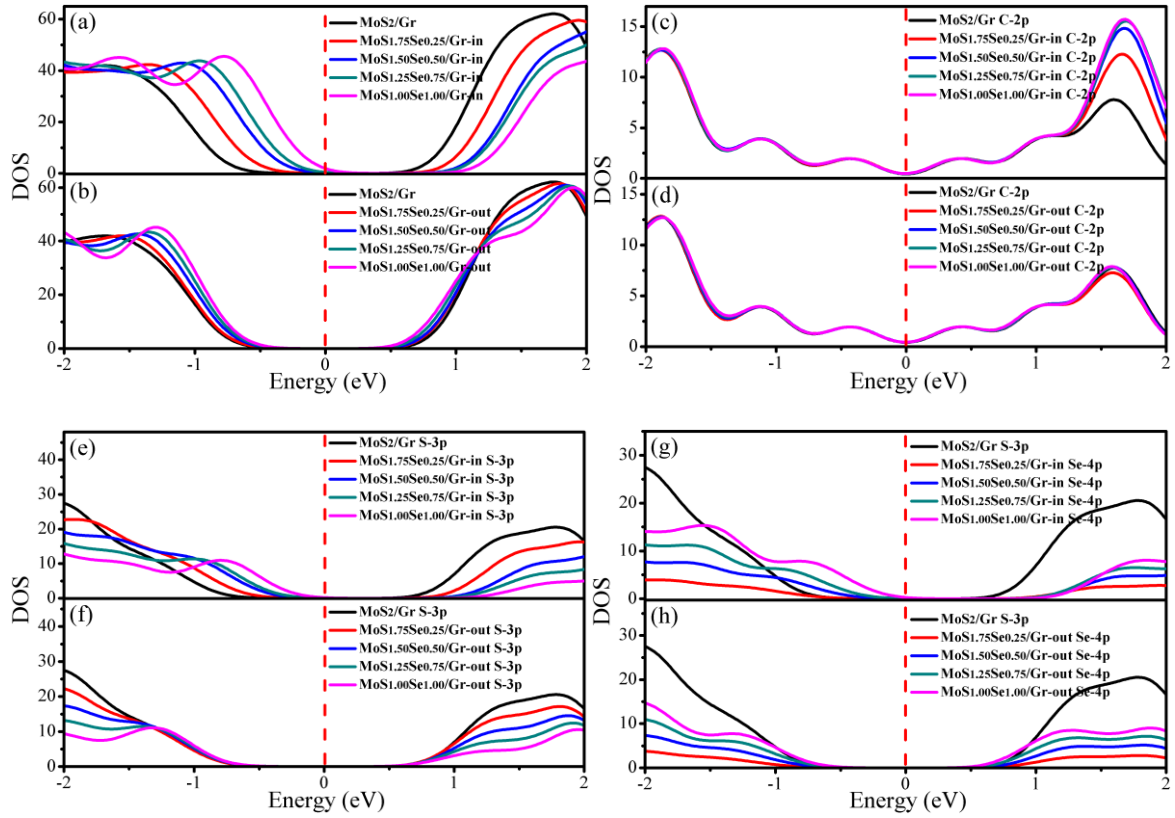

Figure S4. Calculated TDOS of $MoS_{2(1-x)}Se_{2x}$/Gr heterostructure with different Se doping concentration (a) inside and (b) outside the interface. The calculated PDOS of (c) C, (e) S, (g) Se atoms in $MoS_{2(1-x)}Se_{2x}$/Gr heterostructure with different Se dopant concentration inside the interface. The calculated PDOS of (d) C, (f) S, (h) Se atoms in $MoS_{2(1-x)}Se_{2x}$/Gr heterostructure with different Se dopant concentration outside the interface. The vertical line is Fermi level.

5. Interface distance

Table S1. Interface distance at different Se concentrations of $MoS_{2(1-x)}Se_{2x}$/Gr heterostructure.

MoS_2/Gr	$MoS_{1.75}Se_{0.25}$/Gr-in	$MoS_{1.50}Se_{0.50}$/Gr-in	$MoS_{1.25}Se_{0.75}$/Gr-in	$MoS_{1.00}Se_{1.00}$/Gr-in
D=3.406 Å 2.388 Å 2.390 Å	D=3.387 Å D=3.363 Å 2.384 Å 2.495 Å 2.392Å 2.385 Å	D=3.384 Å D=3.356 Å 2.383 Å 2.497 Å 2.387Å 2.386 Å	D=3.381 Å D=3.345 Å 2.378 Å 2.496 Å 2.388Å 2.385 Å	D=3.325 Å 2.487 Å 2.384 Å
	$MoS_{1.75}Se_{0.25}$/Gr-out	$MoS_{1.50}Se_{0.50}$/Gr-out	$MoS_{1.25}Se_{0.75}$/Gr-out	$MoS_{1.00}Se_{1.00}$/Gr-out
	D=3.396 Å D=3.392 Å 2.390 Å 2.389 Å 2.384Å 2.493 Å	D=3.392 ÅD=3.387 Å 2.389 Å 2.388 Å 2.381Å 2.495 Å	D=3.390 ÅD=3.386 Å 2.387 Å 2.390 Å 2.378Å 2.497 Å	D=3.383 Å 2.387 Å 2.493 Å

6. Se dopant atoms on both side of Mo

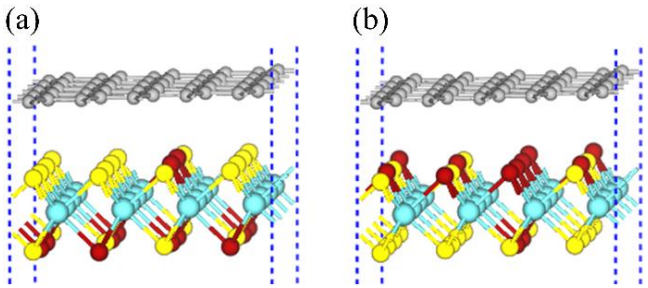

Figure S5. The $MoS_{1.25}Se_{0.75}$/Gr heterostructure with different Se distributions inside or outside interface. Side views of (a) Se inside (x=0.125) and outside (x=0.625) interface, (b) Se inside (x=0.625) and outside (x=0.125) interface. The aquamarinus, yellow, grey, and red balls denote Mo, S, C, and Se atoms, respectively.

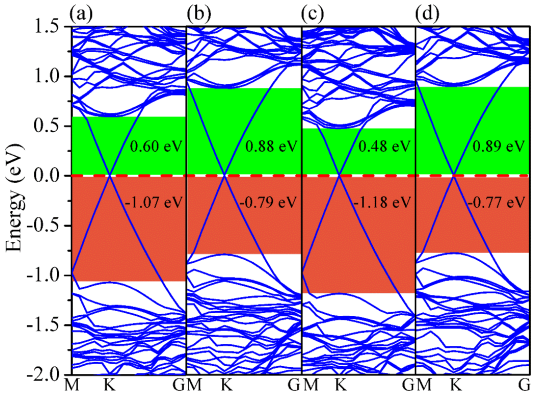

Figure S6. Energy band structures of $MoS_{1.25}Se_{0.75}$/Gr heterostructures with different Se distributions inside or outside interface. (a) Se inside (x=0.125) interface and outside (x=0.625) interface, (b) Se inside (x=0.625) interface and outside (x=0.125) interface, (c) Se outside (x=0.75) interface, (d) Se inside (x=0.75) interface for $MoS_{1.25}Se_{0.75}$/Gr heterostructure, in which green areas and red areas represent n-SBH and p-SBH, respectively. The Fermi level is set to zero and marked by red dotted lines.

7. Electrostatic potentials

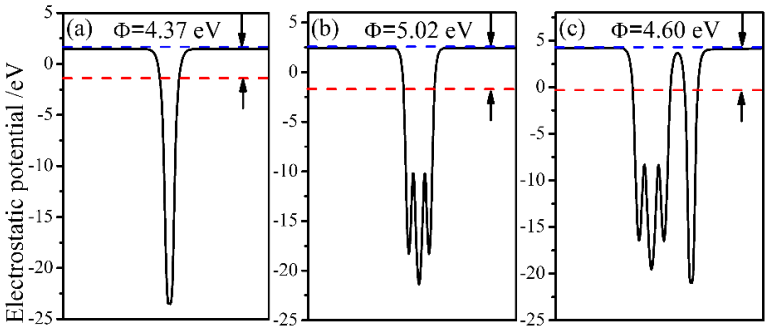

Figure S7. Calculated electrostatic potentials for (a) graphene, (b) monolayer MoS_2, (c) MoS_2/Gr heterostructure.

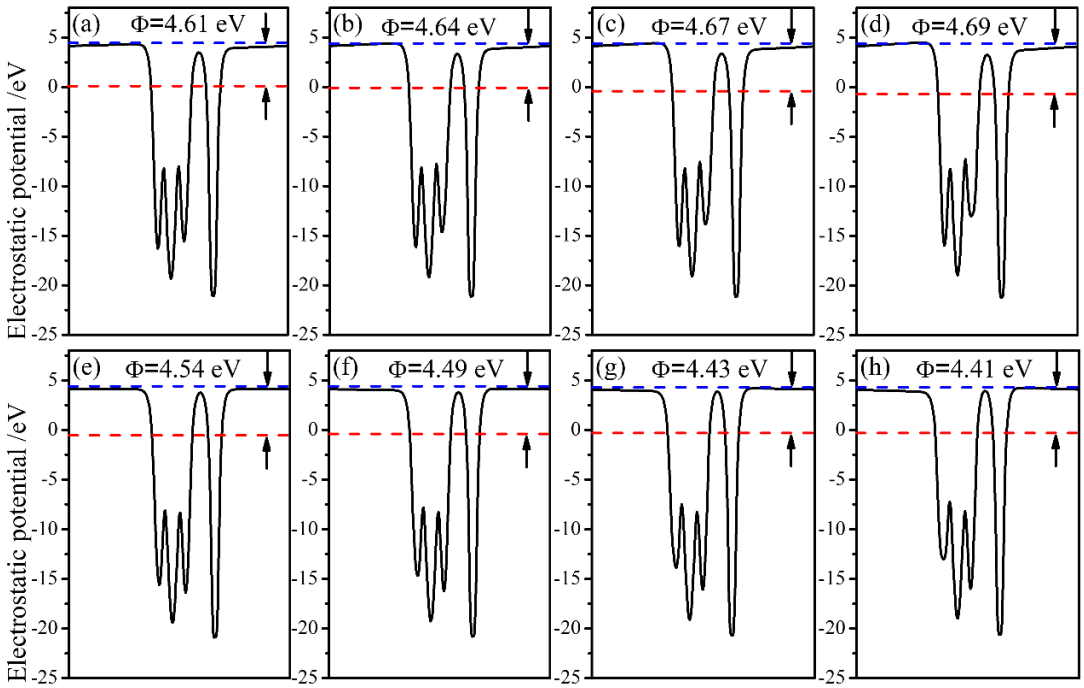

Figure S8. Calculated electrostatic potentials for (a) $MoS_{1.75}Se_{0.25}$/Gr-in, (b) $MoS_{1.50}Se_{0.50}$/Gr-in, (c) $MoS_{1.25}Se_{0.50}$/Gr-in, (d) $MoS_{1.00}Se_{1.00}$/Gr-in; and (e) $MoS_{1.75}Se_{0.25}$/Gr-out, (f) $MoS_{1.50}Se_{0.50}$/Gr-out, (g) $MoS_{1.25}Se_{0.50}$/Gr-out, (h) $MoS_{1.00}Se_{1.00}$/Gr-out. The blue and red dashed lines denote the vacuum energy level and Fermi level, respectively.

8. Three-dimensional (3D) charge density difference

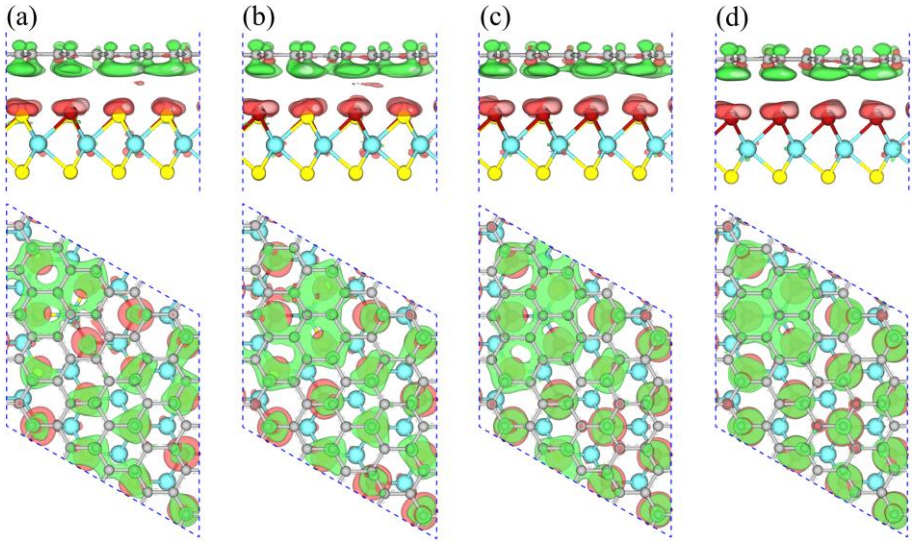

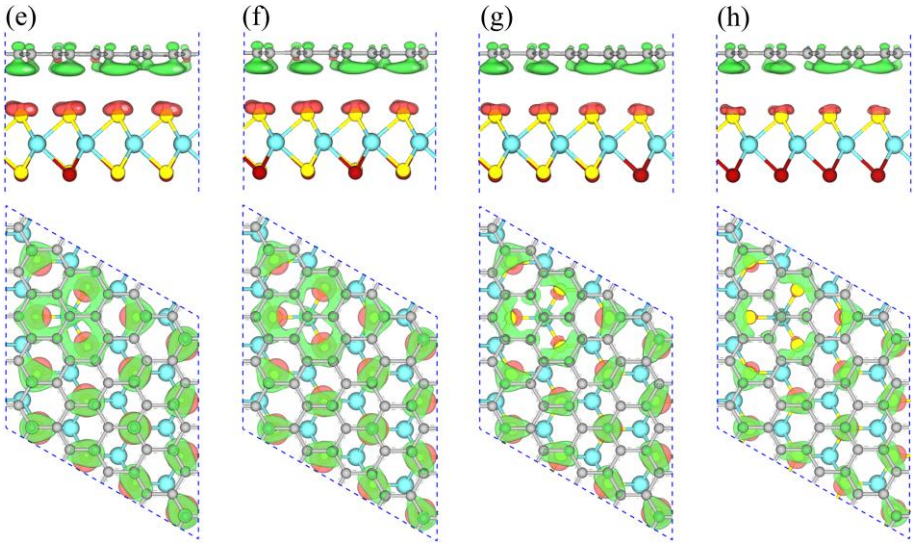

Figure S9. Side and top views of the charge density difference (0.001 e·Å^{-3}) for (a) $MoS_{1.75}Se_{0.25}$/Gr-in, (b) $MoS_{1.50}Se_{0.50}$/Gr-in, (c) $MoS_{1.25}Se_{0.50}$/Gr-in, (d) $MoS_{1.00}Se_{1.00}$/Gr-in, (e) $MoS_{1.75}Se_{0.25}$/Gr-out, (f) $MoS_{1.50}Se_{0.50}$/Gr-out, (g) $MoS_{1.25}Se_{0.50}$/Gr-out and (h) $MoS_{1.00}Se_{1.00}$/Gr-out.